



**HAL**  
open science

# Does Phobos Reflect Solar Wind Protons? Mars Express Special Flyby Operations With and Without the Presence of Phobos

Yoshifumi Futaana, Mats Holmström, Andrey Fedorov, Stas Barabash

► **To cite this version:**

Yoshifumi Futaana, Mats Holmström, Andrey Fedorov, Stas Barabash. Does Phobos Reflect Solar Wind Protons? Mars Express Special Flyby Operations With and Without the Presence of Phobos. Journal of Geophysical Research. Planets, 2021, 126, 10.1029/2021JE006969 . insu-03672355

**HAL Id: insu-03672355**

**<https://insu.hal.science/insu-03672355>**

Submitted on 19 May 2022

**HAL** is a multi-disciplinary open access archive for the deposit and dissemination of scientific research documents, whether they are published or not. The documents may come from teaching and research institutions in France or abroad, or from public or private research centers.

L'archive ouverte pluridisciplinaire **HAL**, est destinée au dépôt et à la diffusion de documents scientifiques de niveau recherche, publiés ou non, émanant des établissements d'enseignement et de recherche français ou étrangers, des laboratoires publics ou privés.



Distributed under a Creative Commons Attribution 4.0 International License

**Key Points:**

- Mars Express identified non-solar wind protons near Phobos during a flyby, possibly from the surface of Phobos
- The protons showed abrupt changes with a time scale of 30 s or a spatial scale of ~70 km
- Special maneuvers of Mars Express rule out possible instrument effects during the Phobos flyby

**Correspondence to:**

Y. Futaana,  
futaana@irf.se

**Citation:**

Futaana, Y., Holmström, M., Fedorov, A., & Barabash, S. (2021). Does Phobos reflect solar wind protons? Mars Express special flyby operations with and without the presence of Phobos. *Journal of Geophysical Research: Planets*, 126, e2021JE006969. <https://doi.org/10.1029/2021JE006969>

Received 4 JUN 2021  
Accepted 21 OCT 2021

## Does Phobos Reflect Solar Wind Protons? Mars Express Special Flyby Operations With and Without the Presence of Phobos

Yoshifumi Futaana<sup>1</sup> , Mats Holmström<sup>1</sup> , Andrey Fedorov<sup>2</sup>, and Stas Barabash<sup>1</sup>

<sup>1</sup>Swedish Institute of Space Physics, Kiruna, Sweden, <sup>2</sup>IRAP, CNRS, Toulouse, France

**Abstract** We characterize the solar wind proton reflection (backscattering) from Phobos using a series of Mars Express operations. The plasma data obtained during the Phobos flyby of Mars Express in January 2016 showed a non-solar wind signal possibly reflected from the Phobos surface. Similar signatures were previously reported during an earlier Phobos flyby in 2008. On the other hand, although Mars Express has encountered Phobos (within 100 km) more than 10 times, it has thus far detected only two clear cases of reflected protons. The intermittency of the reflected proton detections could indicate that these protons are not from Phobos but are produced by the spacecraft body or solar arrays under a special attitude configuration during the flyby maneuver. To rule out these artifacts as the cause, we conducted three special operations; Mars Express was operated using the identical attitude and solar panel control sequence but without Phobos nearby. All the measured plasma data during the special operations exhibit no additional plasma signatures. These *fake flyby* experiments indicate that the measured non-solar wind protons during the real flyby are not from the spacecraft and that Phobos likely reflects solar wind into space. On the other hand, the intermittency of the reflected protons from Phobos remains unexplained. The reflected protons are vital additional plasma components because they inject enough energy to disturb the near-Phobos plasma environment. In addition, we can utilize these reflected particles to remotely measure the surface precipitation flux.

**Plain Language Summary** How does a Martian moon, Phobos, interact with solar wind plasma? Because Phobos lacks an atmosphere and a magnetic field, solar wind plasma directly impacts the surface. The fate of solar wind protons must resemble that of Moon-solar wind interactions. The solar wind protons are reflected back from the lunar surface. Phobos must similarly reflect solar wind protons; however, only two flybys out of dozens of Mars Express flybys have shown such proton reflection. Here, we show the second event in which these ions were detected using a new instrument operation mode. Moreover, to rule out the possibility that the spacecraft body produced such protons, we ran three more “flyby” operations strictly following the attitude control sequence but without Phobos nearby. These “fake flybys” without Phobos prove that the proton signatures measured during the previous actual flybys were not instrument effects produced by the spacecraft body. The reflected proton signatures are different between Phobos and the Moon. Why they are different remains an open question, but the behavior of plasma at the surfaces of these bodies may differ. Because solar wind plasma modifies rocky surfaces in space, the different interactions imply evolution differences between the Moon and Phobos surfaces.

### 1. Introduction

The behavior of Phobos under solar wind plasma has long been an enigma. The outgassing from its surface is expected to be weak, and thus, Phobos does not show “comet-like” interactions. Instead, without a strong magnetic field, Phobos is expected to show “Moon-like” interactions.

Solar wind interaction with the Moon is characterized by direct solar wind plasma precipitation on the surface (Halekas et al., 2011; Holmström et al., 2012; Schubert & Lichtenstein, 1974). Since the Apollo missions, various measurements of the near-Moon environment by many spacecraft have revealed the fundamental physics of the interaction; the Moon absorbs solar wind ions, and a plasma void is formed behind the Moon (Ness et al., 1968). However, measurements and theoretical assessments after 2000 changed the paradigm of Moon-solar wind interactions. Instead of a simple interaction model with the solar wind, the

© 2021. The Authors.  
This is an open access article under the terms of the [Creative Commons Attribution License](https://creativecommons.org/licenses/by/4.0/), which permits use, distribution and reproduction in any medium, provided the original work is properly cited.

actual interaction is highly complicated: namely, the plasma, solid surface, exosphere, and magnetic field actively exchange energy and materials in near-Moon space (Futaana et al., 2018). For example, while the absorption at the lunar surface is thought to be perfect because of the high porosity of the regolith, a significant amount of reflection (backscattering) from its surface has been observed. Saito et al. (2008) discovered protons reflected from the lunar surface with an efficiency of 0.1%–1%. Wieser et al. (2009) and McComas et al. (2009) detected reflected solar wind protons in the form of neutral hydrogen atoms with energies  $\sim 100$  eV (energetic neutral atoms or ENAs). The efficiency of proton reflection in the form of ENAs is 10%–20%. As the total energy of reflected protons is comparable to that of the ambient fields, the reflected protons are capable of exciting instabilities in the electromagnetic field (Futaana et al., 2010). The precipitating solar wind can sputter surface materials, contributing to the formation of the exosphere (Hurley et al., 2016; Stern, 1999; Vorburger et al., 2014; Wurz et al., 2007; Yokota et al., 2020). A local magnetic field of crustal origin can significantly interact with solar wind (Futaana et al., 2003; Lue et al., 2014; Saito et al., 2008; Wieser et al., 2010) and influence the upstream solar wind plasma (Russell & Lichtenstein, 1975). Enormous efforts have been made to simulate the interaction between the Moon and solar wind using a hybrid approach (Fatemi et al., 2015; Holmström et al., 2012; Jarvinen et al., 2014; Poppe, Fatemi, et al., 2016) and a particle (PIC) approach (Bamford et al., 2012; Deca et al., 2015) on both global and local scales. Charged dust also plays a key role in these complicated interactions (Horanyi et al., 2015). These characteristics of the Moon-solar wind interaction could be similar to those of the Phobos plasma environment.

Several Martian orbiters have measured the plasma environment near Phobos in the past. In the 1980s, the Phobos-2 mission carried a comprehensive in situ plasma instrument package including particle, field, and wave instruments together with remote sensing sensors (Sagdeev & Zakharov, 1989). During its elliptical orbits around Mars, disturbances in the electron and ion fluxes, and likely the ion composition, were detected (Dubinin et al., 1990, 1991). Based on the measurement and theoretical estimates, gas and ion tori along the Phobos orbit were proposed (Ip & Banaszekiewicz, 1990; Mura et al., 2002; Sauer et al., 1993; Poppe, Curry, & Fatemi, 2016). However, significant outgassing has not been identified (Fanale & Salvail, 1989). Furthermore, Mars Global Surveyor, equipped with an electron spectrometer (ELS), later identified similar electron flux disturbances regardless of the relative location between Phobos and the spacecraft (Øieroset et al., 2001, 2010). Researchers concluded that the electron disturbances were produced by the Martian bow shock. Using the data from National Aeronautics and Space Administration's Mars Atmosphere and Volatile Evolution mission, Nénon et al. (2019) evaluated the sputtered particle flux, while no plasma signatures directly related to Phobos or its tori have been reported.

The European Space Agency (ESA) Mars Express made several Phobos flybys (Witasse et al., 2014). From the data obtained from the flyby conducted in July 2008, with the closest approach distance of 93 km, we Futaana et al. (2010) reported non-solar wind proton signals. From the observed characteristics combined with intensive test particle trajectory calculations, we concluded that these ions were reflected protons from Phobos. The efficiency was in the range of 0.5%–10%, which is consistent with that for the reflection process measured for the Moon (Saito et al., 2008). We claimed that the reflection process of the solar wind (keV protons) is a general process in space. However, the difference between the reflected ion measurements near Phobos and those of the Moon is that the measured signal near Phobos was intermittent. Proton reflection from the lunar surface is a continuous process (Saito et al., 2008). More surprisingly, reflection has not been detected in many other flybys. Therefore, one of our criticisms of the first detection event in June 2008 was that the detected signal could have been from the spacecraft body or solar arrays. Near the closest approach, the spacecraft made a slew (attitude control maneuver) to point optical instruments at Phobos during the flybys. Because of this special maneuver, solar wind protons may have hit specific places (that no protons can access under the nominal attitude of Mars Express), been reflected, and been detected by the ion mass analyzer (IMA) sensor. In addition to the special spacecraft attitude, a solar array was manipulated. Since the field of view (FOV) of the plasma sensor on Mars Express covers the solar array, there was also a possibility of contamination from reflected solar wind protons. Indeed, the solar array of Venus Express is a possible source of ENAs via the same mechanisms as mentioned above. The solar wind protons hit the solar array, are reflected, and are detected by the ENA sensors. The only difference is that the reflected particles are (positively) charged or neutralized, which is determined stochastically (Eckstein, 1981). Nevertheless, we Futaana et al. (2010) attempted to rule out these criticisms regarding possible artifacts from spacecraft

reflection during the first Phobos flyby by statistically showing that the high proton counts were measured only during the flyby.

In this paper, we report the second clearly detected signals of protons measured during the flyby on January 14, 2016, using a new operation mode of the Mars Express ion instrument. The general characteristics of the second event in 2016 were similar to those of the first event in 2008. These similarities recalled the critiques stating that the signals originate from the spacecraft. To rule out these criticisms, we further conducted three special operations (hereafter called *fake flybys*): The Mars Express was maneuvered using the same attitude and solar panel control sequences, but Phobos was not near the spacecraft. If similar proton signatures were found during the control sequence without Phobos nearby, we can conclude that the signals during the two actual flybys in 2008 and 2016 were artifacts originating from the spacecraft. On the other hand, if there are no signals measured during the fake flybys, the lack of signal would support our previous conclusion that the measured signals were from Phobos. Three fake flyby operations were realized in 2017, and we found no additional plasma disturbances during the fake flybys. These measurements support the argument that the plasma signatures found in the July 2008 and January 2016 flybys were likely from Phobos.

## 2. Instrument

In this study, we used data from the Analyzer of Space Plasma and Energetic Atoms (ASPERA-3) onboard Mars Express (Barabash et al., 2006). The ASPERA-3 instrument is a plasma package comprised of the IMA, the ELS, and two ENA sensors (Neutral Particle Imager and Neutral Particle Detector). We used only the plasma data from the IMA and ELS.

The IMA is a top-hat type electrostatic analyzer for measuring positive ions with moderate mass resolution. The energy range is from 10 eV/q to 32 keV/q, while the default energy range used for the actual operations is narrower (10 eV/q–15 keV/q). The energy range is divided into 96 logarithmically separated steps. The energy setting can be determined by command. The angular coverage is  $\pm 45^\circ$  for the elevation angle, in the direction of electrostatic sweep, with respect to the reference plane, and  $360^\circ$  for the other direction (azimuthal angle, measured instantly). The angular coverage is divided into  $16 \times 16$  bins at maximum, and this is the default setting. Each angular bin has a  $5.6^\circ \times 22.5^\circ$  resolution at the full width at half maximum. The setting of the elevation angle and the binning can also be changed by command. The IMA requires 192 s to measure the ions over the entire energy range and angle coverage by default. This time cadence was far longer than the typical Phobos flyby time scale by Martian orbiters. The relative speed of Mars Express with respect to Phobos was  $\sim 3$  km/s, giving a spatial scale of  $\sim 500$  km for one scan, which is much longer than the spatial scale of Phobos (several tens of km) (Futaana et al., 2010). For the flyby in 2008, we used the nominal time resolution, but the data interpretation was thus not straightforward.

Therefore, we implemented a new mode to improve the IMA time resolution to 24 s. The energy range was restricted to 10 eV/q–3 keV/q with 32 logarithmically separated steps for compensation, while the energy range was optimized to measure the solar wind-related protons. The elevation angle sweep was restricted to six bins ( $\pm 2.8^\circ$ ,  $\pm 8.4^\circ$  and  $\pm 14.0^\circ$  with respect to the reference plane). The corresponding spatial scale of the new 24-s mode was  $\sim 50$  km (the relative speed between the spacecraft and Phobos was 2.1 km/s during the flyby discussed in this paper). This was still greater than the typical Phobos scale, while the new operation mode provided far better performance for characterizing the plasma environment near Phobos. For example, the spacecraft spent  $\sim 1$  min within a distance of 100 km from Phobos. The 24-s time resolution provides almost three full 3D velocity distributions close to Phobos, while the original mode cannot complete a single full scan.

The ELS is a top-hat type electrostatic analyzer for measuring electrons. The ELS was mounted on a scanning platform, while the scanner was not operated during the flybys. The energy range covers 10 eV–20 keV with 128 logarithmically separated steps. The angular coverage is  $5 \times 360^\circ$  with 16 equally separated bins. The time cadence is 4 s for measuring one full energy spectrum.

The Mars Express spacecraft is a 3-D stabilized platform (Figure 1). The IMA instrument is rigidly mounted on the spacecraft. The ELS sensor is mounted on a movable scanner, but the scanner was not in operation during the measurements discussed in this paper. Thus, the ELS was mounted rigidly on the spacecraft in

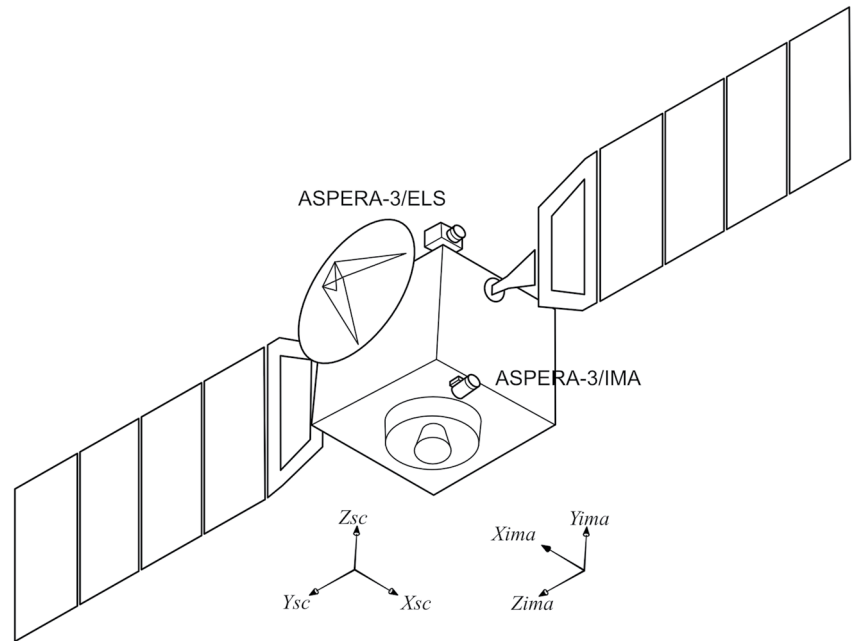


**Figure 1.** Analyzer of Space Plasma and Energetic Atoms (ion mass analyzer and electron spectrometer [ASPERA-3/ELS] accommodation on a simplified illustration of the Mars Express spacecraft. The coordinate systems used in this study are also shown.

practice. In this paper, the attitude of the spacecraft was represented by two angles with respect to the Sun direction (approximately parallel to the solar wind impingement direction):  $EL = \cos^{-1}n_z$  and  $AZ = \tan^{-1}n_y/n_x$ , where  $(n_x, n_y, n_z)$  is the Sun direction in the IMA reference frame. The geometry of the Sun direction represents where the solar wind protons came from in the spacecraft and IMA instrument's reference frame. The largest movable structures on the spacecraft are its solar arrays. The solar arrays are mounted on the  $\pm y$ -plane of the spacecraft and rotate around the  $y$ -axis. The rotation angle is thus another parameter that can determine the geometry of the proton measurement via the change in the envelope of the spacecraft shape.

### 3. Phobos Flyby and Plasma Measurement

#### 3.1. Phobos Flyby in 2016 and Comparison With the Previous Event

Figure 2 shows the flyby geometry on January 14, 2016. The flyby occurred in the solar wind, and the closest approach of Mars Express to Phobos occurred at 16:00:24, with a distance of  $\sim 57$  km from the center. Phobos (and Mars Express) was located far upstream of the bow shock. The distance to the bow shock surface was 2,000 km, which is longer than the typical proton gyroradius of 1,000 km (for a typical IMF strength of 3 nT and proton speed of 400 km/s). The ion signatures were sporadic, seen only close to Phobos, and did not continue to the bow shock surface. Although we cannot confirm conclusively from the data, the measured signals are unlikely to be a part of the ion foreshock populations. Foreshock electrons could be measured if the magnetic field was directly connected to the shock surface. During the flyby, Mars Express conducted an attitude control maneuver for Phobos observations. The maneuver was driven by the other optical instruments on Mars Express. During the flyby, ASPERA-3/IMA used the newly implemented 24-s mode. The ion and electron energy-time spectra are shown in Figure 3. The IMA energy range was limited to 10–3,000 eV/q with only six elevation channels (Figures 3c–3h) but provided a 24 s time resolution. The ELS was operated at the nominal 4 s time resolution.

The solar wind proton and alpha particles can clearly be seen at an elevation angle close to  $0^\circ$  (Figures 3e and 3f) at 15:30 (at  $E/q \sim 2$  keV for protons and  $E/q > \sim 3$  keV for alpha particles). The spacecraft was in the solar wind, outside of the Martian bow shock (Figure 2a). Because of the spacecraft maneuver, the incident

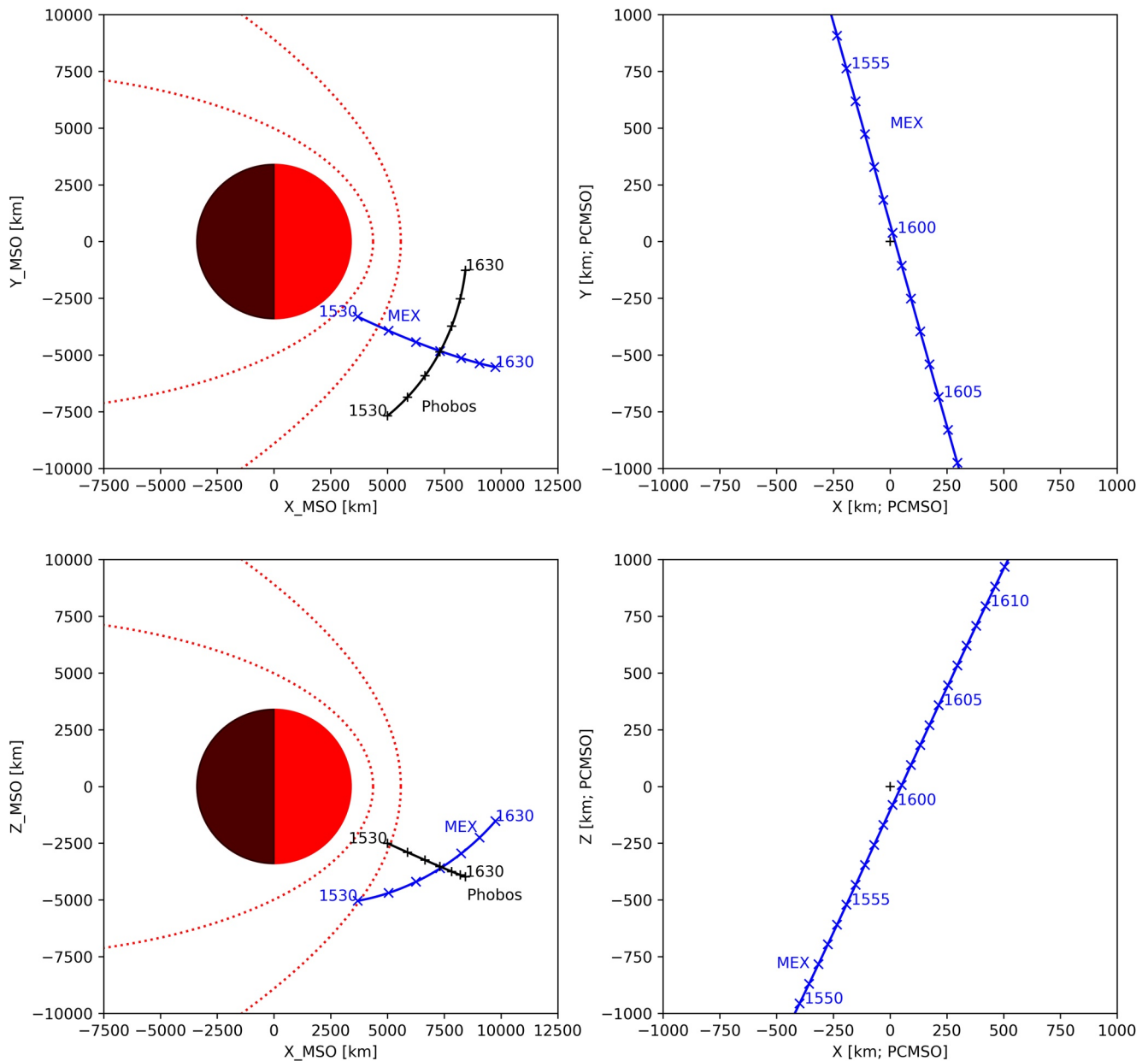


**Figure 2.** The geometry of the Mars Express' Phobos flyby on January 14, 2016 (orbit number 15260). (Left) The Mars Express (blue) and Phobos (black) orbits with respect to the Martian plasma environment (the bow shock and magnetic pileup boundary are represented by dashed curves; Vignes et al. (2000)). The MSO (Mars Solar Orbit) reference frame is used, where  $x$  points from Mars to the Sun,  $y$  points opposite to the Mars orbital velocity vector, and  $z$  completes the right-hand system. (Right) The Mars Express orbit centered at the Phobos body. The MSO axes were used but the origin is Phobos (PCMSO; Phobos-Centered MSO).

solar wind was directed toward lower elevation channels in the IMA fixed reference frame (Figures 3g and 3h). The solar wind moved outside of the IMA FOV between 15:42 and 16:00. The solar wind signal reentered the FOV at ~16:00 and then moved toward higher elevation angle channels (Figures 3c and 3d). After 16:15, the solar wind moved back to the central channels (Figures 3e and 3f), that is, the nominal attitude of Mars Express. The time series of the solar wind incident angle is shown in Figure 3b, where the total counts registered were integrated over the angle and energy. Figure 3b further overlays the Sun direction on the IMA instrument reference frame (the elevation angle). The solar wind incident angle followed the Sun direction in the IMA reference frame, indicating that the solar wind was undisturbed.

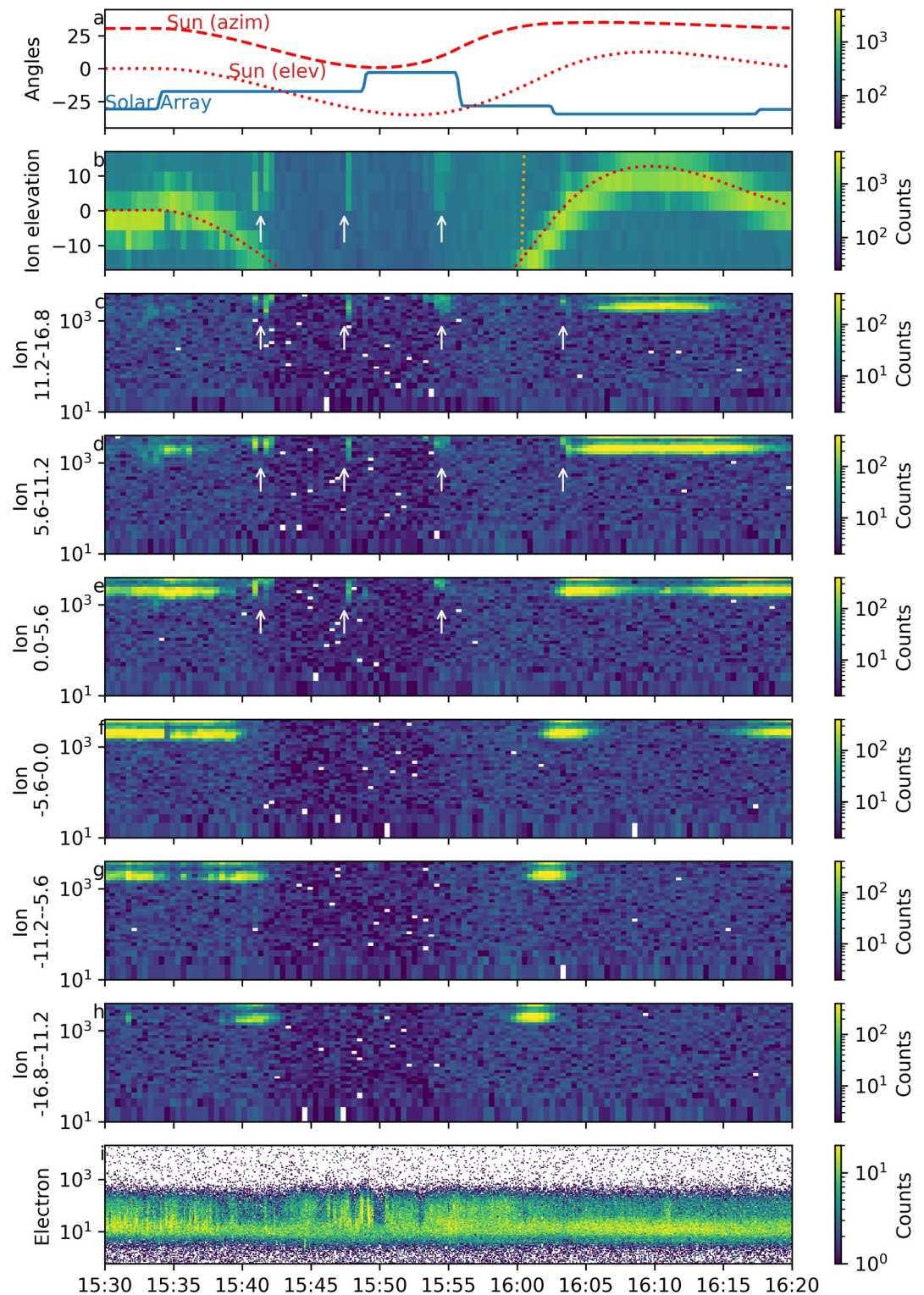


**Figure 3.** Plasma measurements by Mars Express/Analyzer of Space Plasma and Energetic Atoms (ASPERA-3) during the Phobos flyby on January 14, 2016. (a) The solar array angle (blue) with respect to a reference position and the Sun direction in the Ion Mass Analyzer (IMA) reference frame (the elevation and azimuthal angles). (b) The time series of the ion counts measured by ASPERA-3/IMA represented in the format of the elevation angle-time diagram. The red dot curve shows the Sun direction in the IMA reference frame (the elevation angle as in panel (a)). (c–h) Energy-time diagram for six elevation channels. (i) Electron energy-time diagram measured by ASPERA-3/electron spectrometer.

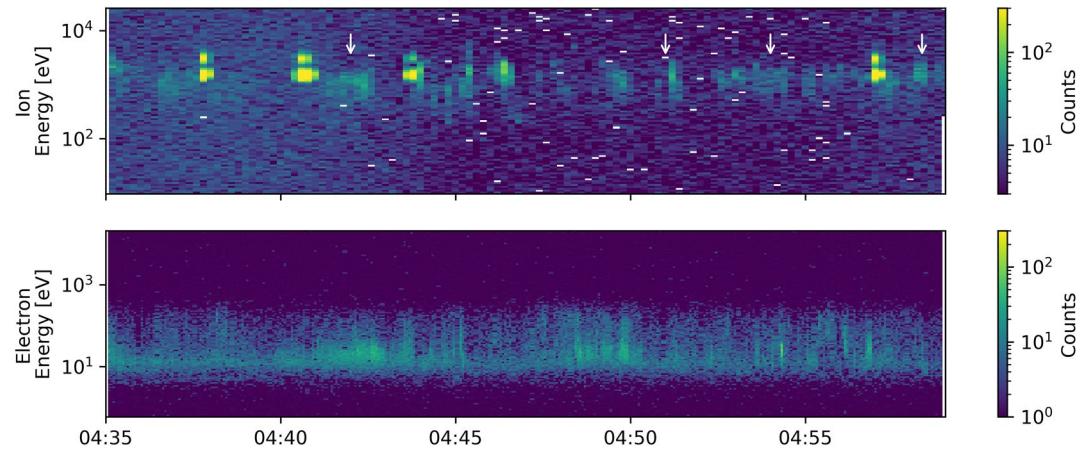


**Figure 4.** Ion and electron data measured during the flyby on July 23, 2008 (orbit number 5851). The closest approach to Phobos was 93 km at 04:50. Intermittent signatures of solar wind protons that came from Phobos were observed (white arrows) (Futaana et al., 2010).

In addition to the solar wind protons and alpha particles, non-solar wind signals are seen sporadically at 15:40, 15:48, 15:55, and 16:03 (Figures 3c–3e). The characteristics of these signals were similar to what was observed during the Phobos flyby in July 2008 (Figure 4) from various perspectives: (a) the energy was very similar to or occasionally exceeded the solar wind energy; (b) the ion composition was only protons (Figure 5); (c) the signals were measured only near Phobos (<1000 km); (d) the signals appeared intermittently in time; and (e) the signals did not necessarily come from the direction of Phobos (because the electromagnetic fields influenced the proton trajectories), as shown in Figure 6a. These common features led us to conclude that the measured protons in January 2016 were the second clear case of reflected protons from Phobos.

The newly implemented 24-s mode provides updated information about the reflected protons from Phobos. In the previous flyby in 2008 using the nominal 192-s mode, we proposed that the sporadic features could be due to the insufficient time resolution of the IMA operation (192 s). The long instrument sweep in energy and direction, and the fast motion of the spacecraft caused a change in the geometry during a measurement. However, even when we used the higher time-resolution mode (24 s), sporadic features remained, implying that the intermittent features are intrinsic. We can restrict the temporal or spatial scales from the measurements to be the time scale of ~20 s, corresponding to ~50 km.

One of the possible sources of these protons is the spacecraft body or solar array. As seen in Figure 6a, the signals came from close to the solar panel. As the IMA is mounted on a spacecraft, a part of its FOV unavoidably includes the spacecraft body. However, this hypothesis is an unlikely explanation for the measured characteristics of the protons. The energy of the non-solar wind signal can reach higher energy than the nominal solar wind (Figure 6b). Considering the energy loss during the surface interaction, the measured energy of ions should not exceed the original solar wind energy at birth. Due to the very short travel distance from a part of the spacecraft to the IMA sensor (less than a meter), such ions cannot obtain enough energy from the ambient electric field or the spacecraft potential. Furthermore, we Futaana et al. (2010) surveyed all available IMA data to determine whether similar proton signals are statistically coming from the same direction (i.e., from the direction close to the solar panel) to validate if the measured protons are of spacecraft origin. We found that significant proton counts from the solar panel direction were measured only during the Phobos flyby. These arguments support our conclusion that the measured plasma signature is not an artifact from the spacecraft. To further experimentally invalidate the influence of the spacecraft, we conducted special operations as described in the following section.

### 3.2. Fake Phobos Flybys of Mars Express

Special operations, *fake flybys*, were implemented with the assistance of the Mars Express operation team at the ESA in 2017. The purpose of the fake flybys is to assess the spacecraft influence on potential ion

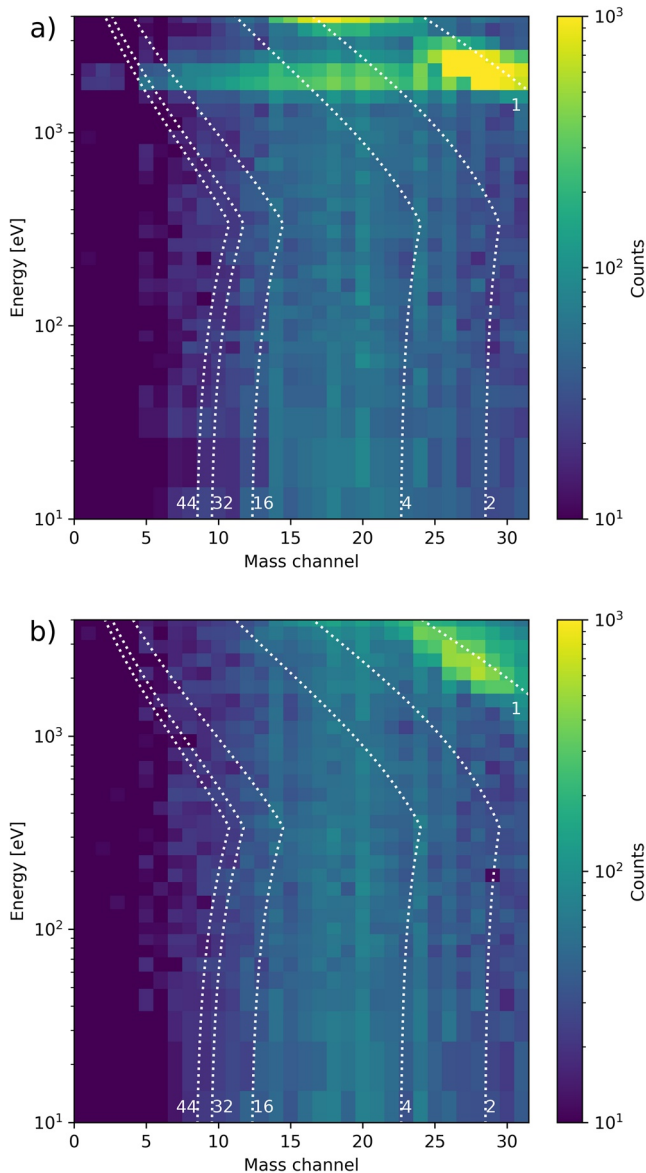


**Figure 5.** The energy-mass matrixes of the measured ions for (a) the solar wind composition (accumulated counts for the elevation angle  $> 0$ , Figures 4c–4e, between 15:38:20 and 16:03:32) and (b) the non-solar wind composition (accumulated counts for elevation angle  $< 0$ , Figures 4f–4h, in the same time period). The dotted curves represent the mass-per-charge contour curves for  $M/q = 1, 2, 4, 16, 32,$  and  $44$ . Solar wind protons are seen clearly in panel (a) at 2 keV, with extended band-like noise in the higher mass channel (sometimes referred to as the ghost). Alpha particles are seen at the highest energy step ( $\sim 4$  keV). The non-solar wind composition includes only protons.

production during a flyby maneuver. The Mars Express operation sequence identical to the period of the Phobos flyby, including the attitude control maneuver and the solar array operations, was used when the spacecraft was located in the solar wind but far from Phobos. Three fake flyby operations were conducted. Figure 7 shows the geometry of the second flyby.

Figure 8 shows the energy-time diagram measured during the second fake flyby. The maneuver operation was successfully completed. Figure 8a shows that the spacecraft attitude angles and the solar array setting varied over time, the same as in the real flyby (Figure 3a). Figure 8b shows that the change in the elevation channels of the impinging solar wind protons varied in the same manner as that of the real flyby in 2016 (Figure 3b). The solar wind came from the Sun direction, as expected, and the time sequence of the solar wind direction in the IMA reference frame was consistent with that of the real flyby. On the other hand, no additional signatures were detected during the fake flyby (Figure 8) in contrast to the real Phobos flyby (Figure 3). No disturbances in the electron data can be identified. The first (May 17, 2017, 0410–0440) and third (May 21, 2017, 0600–0630) fake flyby data did not show any ion populations other than the undisturbed solar wind.

#### 4. Discussion and Concluding Remarks

Mars Express has regularly conducted Phobos flybys since its orbit insertion around Mars in 2003 (Witasse et al., 2014). During the 2008 flyby (with the closest approach at 93 km), keV-energy non-solar wind protons were detected, and we (Futaana et al., 2010) concluded that these protons were reflected solar wind from Phobos.

The interaction between Phobos and the solar wind should resemble that of the Moon-solar wind interactions since these two bodies do not possess an atmosphere. Because of the lack of atmosphere, solar wind protons can access the surfaces of these bodies. At the lunar surface, solar wind protons are continuously reflected back in the form of protons (Saito et al., 2008) and ENAs (McComas et al., 2009; Wieser et al., 2009) with energies on the order of 100 eV (Futaana et al., 2012; Lue et al., 2014). Therefore, a similar interaction is expected near Phobos, yet only a single measurement has previously demonstrated a possible signal from ions coming from Phobos (Futaana et al., 2010).

The new measurement near Phobos by Mars Express ASPERA-3 in 2016 reported in this paper (Figure 3) provides an additional event of non-solar wind protons near Phobos. Furthermore, the fake flyby operations conducted in 2017 (Figure 8) provide evidence that the measured protons are not produced locally by the spacecraft body or solar array.

On the other hand, we have seen such ion beams in only two orbits out of more than a dozen Phobos flybys. Even in the two clearly identified events, the proton signatures are sporadic. More recent flybys in 2019 and 2020 in similar configurations did not show any signatures. The question of why the protons from Phobos are sporadic remains open.

Hypotheses that potentially solve the enigma are as follows:

- The temporal and spatial scales of Phobos are much smaller than those of the measurements. Even with the newly implemented 24-s mode, we could not obtain the full 3-D velocity distribution fast enough,

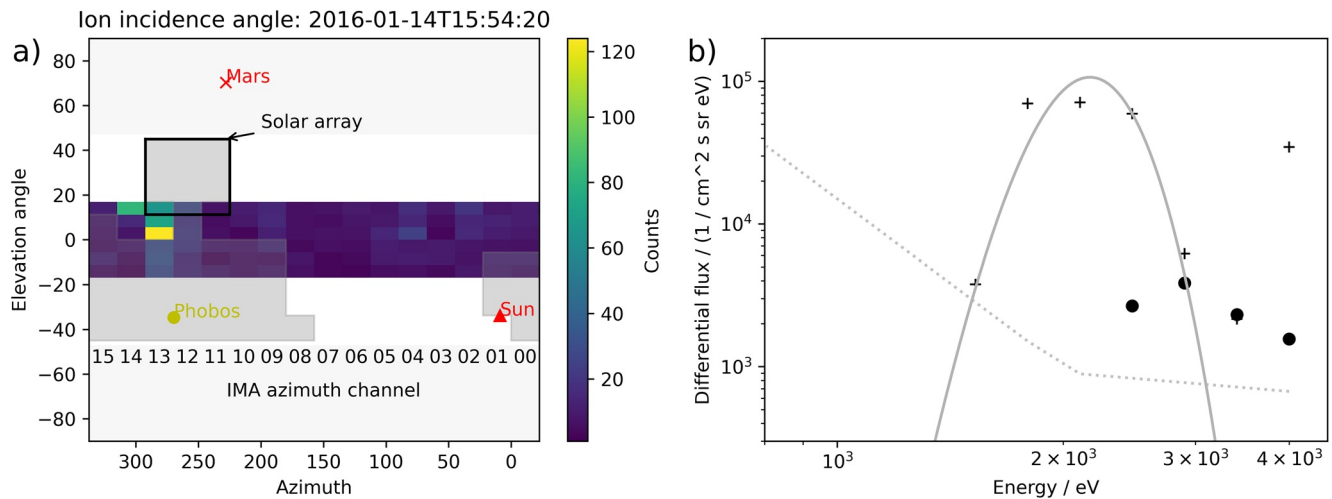


**Figure 6.** (a) The angular response of the Phobos-related protons measured during the real flyby on January 14, 2016. The signal mainly came from the azimuthal angle of 280°, corresponding to azimuthal channel 13. (b) The energy spectra of ions measured by the ion mass analyzer during the real flyby. Data points marked by + represent the undisturbed solar wind (Figure 5a, both protons and alpha particles), and those with · are the non-solar wind protons, possibly from Phobos. Maxwellian fitting for the solar wind protons is shown by the gray curve. The dashed curve is the instrument one-count level.

as the IMA should scan its elevation angle and energy within the period. In 24-s, the spacecraft moved ~50 km. In addition, the scale of Phobos (~10 km) indicates that the volume in the 6-dimensional phase space that reflected ions can fill could be very small and highly variable due to the interplanetary magnetic field direction. If this is the case, more observations near Phobos will be helpful.

- Electric or magnetic fields can interfere with solar wind precipitation on the Phobos surface. If Phobos is magnetized due to crustal magnetic fields or global induced fields (Mordovskaya et al., 2001), the solar wind cannot reach the surface. If this is the case, proton reflection would not occur. Such a change in the reflection of protons due to magnetization has been seen on the Moon (Wieser et al., 2010), while clear evidence of global or local magnetization at the Phobos surface has not been observed.
- The Phobos regolith has different characteristics than the lunar regolith in terms of the interaction with solar wind protons due to, for example, the differences in gravity or distance from the Sun. If highly localized regions with high and low efficiencies exist, then the proton signatures measured by a spacecraft could be intermittent. Asymmetry between the near- and far-sides may exist (Nénon et al., 2021). On the other hand, the efficiency of the reflected particles is known to be independent of the lunar surface characteristics in the case of the Moon (Vorburger et al., 2013). Further experimental and theoretical assessments are necessary for a solid discussion.
- Small-scale geographical structures may absorb the reflected proton trajectories or induce local electric field structure disturbances due to the different illumination conditions (Farrell et al., 2010) affecting the trajectory of the reflected protons.
- The measured signals came from the Martian bow shock. This explanation is possible, but we consider it unlikely for the following reasons. The signal was sporadic and found only close to Phobos. If the spacecraft was in the foreshock region, the ion signal is expected to have been stable longer, possibly extending to the bow shock (Yamauchi et al., 2011). The measured ion beam's incident direction was ~90° away from the direction of Mars, and the protons show a beam-like structure, not a ring-like structure. A more detailed systematic study of ion velocity distribution in the foreshock region would help interpret the observations more robustly in the future. Even if the measured signal (Figure 3) turns out to be from the bow shock in the future, the question raised in this paper (*Does Phobos reflect solar wind protons?*) remains unanswered, and the discussion in this paper is still valid.
- The measured signals during the two flybys were due to unidentified instrumental effects. One concern with the data is that the measured signals came from a similar direction (around azimuthal sector CH-13) (Figure 6). While the influence of the spacecraft body was excluded by the fake flyby operations, there may be electronic noise that could produce such a signal. In particular, CH-13 has a relatively high sensitivity for background counts, approximately three times higher background counts than the

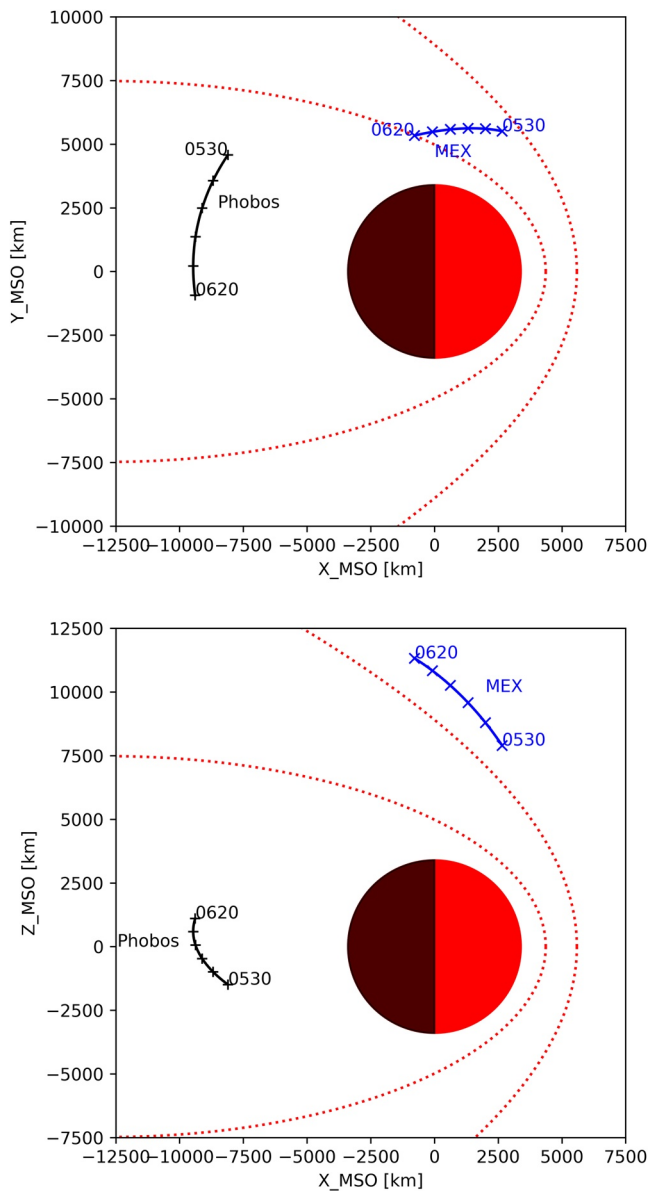


**Figure 7.** The geometry of the second fake flyby on May 19, 2017 (0530–0620 UTC) (orbit number 16943). Mars Express was in the solar wind, and Phobos was located far away downtail of Mars. The dashed black curve represents the orbit of Phobos in the cylindrical projection.

adjacent channels. However, the intense background counts cannot explain the measured signals because the signals are from protons, not background (Figure 4).

Overall, the intermittently measured protons during Phobos flybys are likely coming from the Phobos surface, but other possibilities have not been excluded. However, the fake flybys of Mars Express and analysis in this paper have notably progressed our understanding by explicitly showing that the protons measured during Phobos flybys are not from reflected protons from the spacecraft body.

Further, flyby data combined with global simulations of Phobos-solar wind interactions would provide clues to answer this open question. Ground-based laboratory measurement of proton irradiation on lunar or Phobos samples (and simulants) may be an intriguing future experiment. In addition, the next Phobos mission, JAXA’s Mars Moon Explorer (MMX) mission, is equipped with a highly capable ion sensor named Mass Spectrum Analyzer (MSA). With the quasi-stationary orbit of the MMX, the Phobos-solar wind interaction can be monitored with almost zero relative velocity. These measurements are highly desirable for characterizing the solar wind proton behavior near Phobos to explain the Phobos-solar wind interaction and, more generally, to explain the regolith-plasma interaction in space.

The reflected protons (and ENAs) were first measured only a decade ago, and the regolith-plasma interaction is not yet fully understood. For example, it is known that a rough surface does not efficiently reflect an incoming ion beam from laboratory experiments. In fact, solar wind protons have been thought to be absorbed fully at the surface (Crider & Vondrak, 2002). The physical mechanism of a highly efficient reflection rate (0.5%–1% for protons and 10%–20% for neutral hydrogen) remains an open question. In addition to the fundamental physics, the reflected particles can be used to diagnose the surface-solar wind interaction. The number of solar wind protons that actually bombard the surface is vital information for assessing space weathering effects on the surface. This is also significantly associated with the hydrogen balance at the top surface of celestial bodies. For example, impinging protons may be converted to hydroxyl groups, which can eventually be converted to water (Benna et al., 2019; Ichimura et al., 2012). The momentum of the solar wind deposited on the surface can sputter the surface materials of celestial bodies. These sputtered materials are a significant source of the exosphere (Wurz et al., 2007). Furthermore, the long-term erosion of the surface materials to plasma influences the surface characteristics (weathering). These phenomena are parts of complex systems of celestial bodies’ interactions with the space environment (Futaana et al., 2018). Measurements of the

solar wind flux impinging on the surface provide critical information for understanding complex systems. As the reflected particles can characterize the impinging proton flux at the surface from the orbiter (Futaana et al., 2006, 2013; Wieser et al., 2010), the reflected particle measurements open a new pathway for remotely measuring the solar wind proton characteristics impinging on a surface in space. This technique can be applied to other airless bodies such as Mercury (with the BepiColombo mission; Saito et al., 2010, 2021) and the Jovian moons.

In the end, we emphasize the uniqueness of the “fake flyby” operations. It has been common for optical instruments to point to well-characterized objects for calibration and characterization. On the other hand, thanks to the wide FoVs of plasma particle instruments in general and the relatively wide velocity distribution of space plasma, plasma instrument operation teams (including scientists) do not request spacecraft

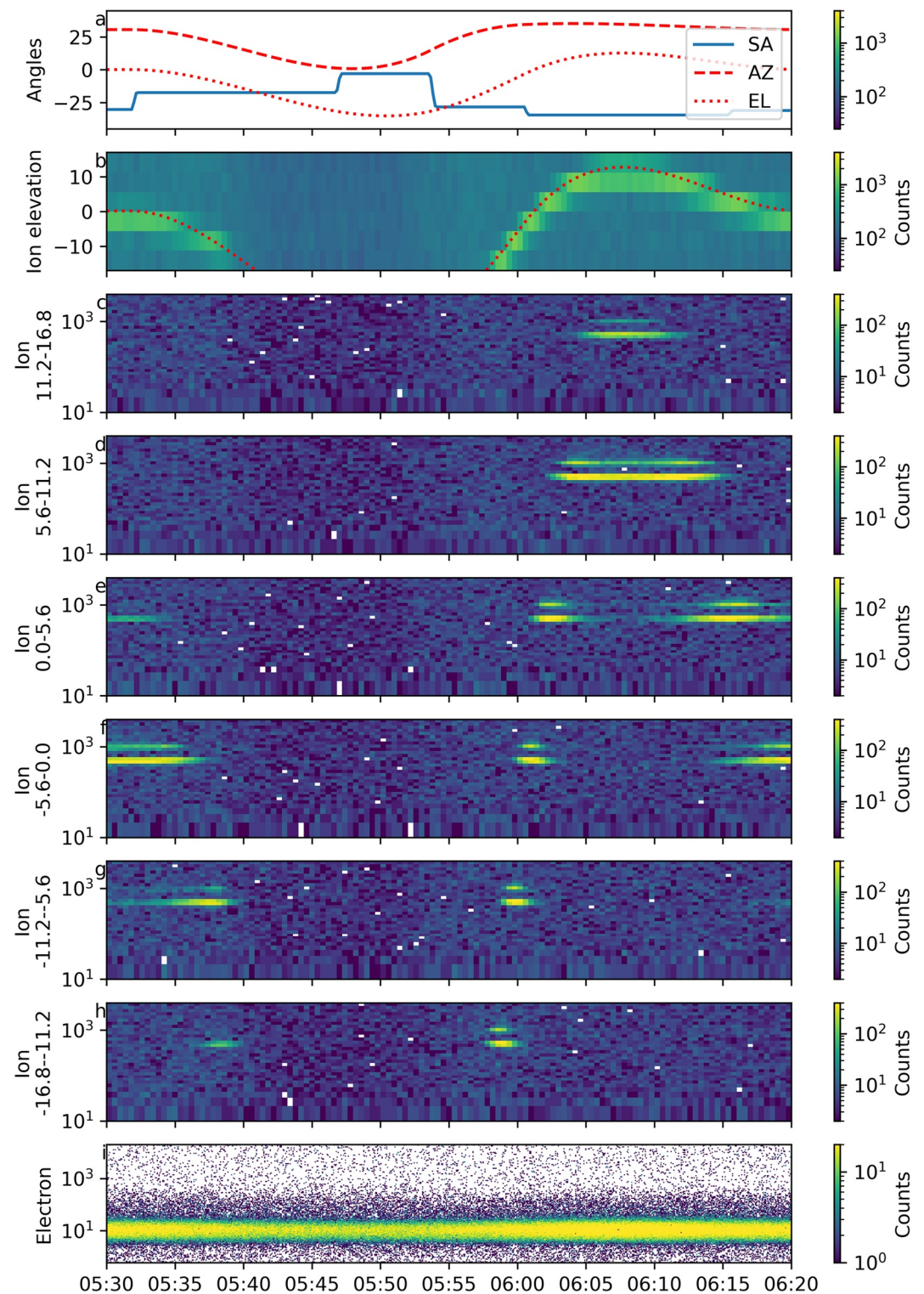


**Figure 8.** Energy-time diagram during the second Phobos fake flyby (on May 19, 2017) in the same format as Figure 3.

pointing. However, we show that the fake flyby operation provided an opportunity for “control experiments” and produced a valuable data set to rule out the possible spacecraft effect during the Phobos flybys. To our knowledge, it is not very easy to obtain such control experiments for space plasma experiments because the environment of interest is highly variable, both in space and time. Indeed, this was the Mars Express

ASPERA-3 operation team's first, and to date only requirement on the spacecraft pointing. In future missions, a similar technique can be used to understand the plasma-spacecraft interactions, such as how irradiated protons interact with the spacecraft. Similar experiments possibly provide opportunities to derive the differential spacecraft potential distribution under different solar photon and plasma incident directions. Such interactions are difficult to characterize during the ground calibration campaign, and therefore we usually rely on computer simulations (Bergman et al., 2020).

## Data Availability Statement

All the data used in this study can be obtained from the FAIR-complied NASA Planetary Data System (PDS) ([https://pds-geosciences.wustl.edu/missions/mars\\_express/aspera.htm](https://pds-geosciences.wustl.edu/missions/mars_express/aspera.htm)). Identical data are also available from the Planetary Science Archive (PSA; <https://www.cosmos.esa.int/web/psa/mars-express>) and the SPICE kernel repository (<https://www.cosmos.esa.int/web/spice/home>) at ESA. The data used in this study are the raw (EDR) data in the PDS/PSA archives. The product names are MEX-M-ASPERA3-2-EDR-ELS-EXT2-V1, MEX-M-ASPERA3-2-EDR-ELS-EXT5-V1, MEX-M-ASPERA3-2-EDR-ELS-EXT6-V1, MEX-M-ASPERA3-2-EDR-IMA-EXT2-V1.0, MEX-M-ASPERA3-2-EDR-IMA-EXT5-V1.0, and MEX-M-ASPERA3-2-EDR-IMA-EXT6-V1.0. The data plotted in each figure are available in the Zenodo repository (Futaana et al., 2021).

## Acknowledgments

ASPERA-3 was supported by the efforts of 14 institutes from 15 countries. A part of the Swedish contribution to the ASPERA-3 instrument development and operation at IRF as the Principal Investigator institution was supported by the Swedish National Space Board. The special maneuvers of Mars Express were supported by the Science Working Team of Mars Express. The authors also appreciate the scientists and engineers at the ESTEC, ESOC, and ESAC who devoted their efforts toward realizing the special operations dedicated to this study.

## References

- Bamford, R. A., Kellett, B., Bradford, W. J., Norberg, C., Thornton, A., Gibson, K. J., et al. (2012). Minimagetospheres above the lunar surface and the formation of lunar swirls. *Physical Review Letters*, *109*, 081101. <https://doi.org/10.1103/PhysRevLett.109.081101>
- Barabash, S., Lundin, R., Andersson, H., Brinkfeldt, K., Grigoriev, A., Gunell, H., et al. (2006). The Analyzer of Space Plasmas and Energetic Atoms (ASPERA-3) for the Mars Express mission. *Space Science Reviews*, *126*(1), 113–164. <https://doi.org/10.1007/s11214-006-9124-8>
- Benna, M., Hurley, D. M., Stubbs, T. J., Mahaffy, P. R., & Elphic, R. C. (2019). Lunar soil hydration constrained by exospheric water liberated by meteoroid impacts. *Nature Geoscience*, *12*(5), 333–338. <https://doi.org/10.1038/s41561-019-0345-3>
- Bergman, S., Stenberg Wieser, G., Wieser, M., Johansson, F. L., & Eriksson, A. (2020). The influence of spacecraft charging on low-energy ion measurements made by RPC-ICA on Rosetta. *Journal of Geophysical Research: Space Physics*, *125*(1), e2019JA027478. <https://doi.org/10.1029/2019JA027478>
- Crider, D. H., & Vondrak, R. R. (2002). Hydrogen migration to the lunar poles by solar wind bombardment of the Moon. *Advances in Space Research*, *30*(8), 1869–1874. [https://doi.org/10.1016/S0273-1177\(02\)00493-3](https://doi.org/10.1016/S0273-1177(02)00493-3)
- Deca, J., Divin, A., Lembège, B., Horányi, M., Markidis, S., & Lapenta, G. (2015). General mechanism and dynamics of the solar wind interaction with lunar magnetic anomalies from 3-D particle-in-cell simulations. *Journal of Geophysical Research*, *120*(8), 6443–6463. <https://doi.org/10.1002/2015JA021070>
- Dubinin, E. M., Lundin, R., Pissarenko, N. F., Barabash, S. V., Zakharov, A. V., Koskinen, H., et al. (1990). Indirect evidences for a gas/dust torus along the Phobos orbit. *Geophysical Research Letters*, *17*(6), 861–864. <https://doi.org/10.1029/g1017i006p00861>
- Dubinin, E. M., Pissarenko, N. F., Barabash, S. V., Zakharov, A. V., Lundin, R., Pellinen, R., et al. (1991). Plasma and magnetic field effects associated with Phobos and Deimos tori. *Planetary and Space Science*, *39*(1–2), 113–121. [https://doi.org/10.1016/0032-0633\(91\)90133-u](https://doi.org/10.1016/0032-0633(91)90133-u)
- Eckstein, W. (1981). Charge fractions of reflected particles. In E. Taglauer, & W. Heiland (Eds.), *Inelastic particle-surface collisions* (pp. 157–183). Springer Berlin Heidelberg. [https://doi.org/10.1007/978-3-642-87065-1\\_11](https://doi.org/10.1007/978-3-642-87065-1_11)
- Fanale, F. P., & Salvail, J. R. (1989). Loss of water from Phobos. *Geophysical Research Letters*, *16*(4), 287–290. <https://doi.org/10.1029/g1016i004p00287>
- Farrell, W. M., Stubbs, T. J., Halekas, J. S., Killen, R. M., Delory, G. T., Collier, M. R., & Vondrak, R. R. (2010). Anticipated electrical environment within permanently shadowed lunar craters. *Journal of Geophysical Research*, *115*(E3). <https://doi.org/10.1029/2009JE003464>
- Fatemi, S., Lue, C., Holmström, M., Poppe, A. R., Wieser, M., Barabash, S., & Delory, G. T. (2015). Solar wind plasma interaction with Gerasimovich lunar magnetic anomaly. *Journal of Geophysical Research*, *120*(6), 4719–4735. <https://doi.org/10.1002/2015JA021027>
- Futaana, Y., Barabash, S., Holmström, M., & Bhardwaj, A. (2006). Low energy neutral atoms imaging of the Moon. *Planetary and Space Science*, *54*(2), 132–143. <https://doi.org/10.1016/j.pss.2005.10.010>
- Futaana, Y., Barabash, S., Holmström, M., Fedorov, A., Nilsson, H., Lundin, R., et al. (2010). Backscattered solar wind protons by Phobos. *Journal of Geophysical Research*, *115*(A10). <https://doi.org/10.1029/2010JA015486>
- Futaana, Y., Barabash, S., Wieser, M., Holmström, M., Lue, C., Wurz, P., et al. (2012). Empirical energy spectra of neutralized solar wind protons from the lunar regolith. *Journal of Geophysical Research*, *117*(E5). <https://doi.org/10.1029/2011JE004019>
- Futaana, Y., Barabash, S., Wieser, M., Lue, C., Wurz, P., Vorburger, A., et al. (2013). Remote energetic neutral atom imaging of electric potential over a lunar magnetic anomaly. *Geophysical Research Letters*, *40*, 262–266. <https://doi.org/10.1002/grl.50135>
- Futaana, Y., Barabash, S., Wieser, M., Wurz, P., Hurley, D., Horányi, M., et al. (2018). SELMA mission: How do airless bodies interact with space environment? The Moon as an accessible laboratory. *Planetary and Space Science*, *156*, 23–40. <https://doi.org/10.1016/j.pss.2017.11.002>
- Futaana, Y., Holmstrom, M., Fedorov, A., & Barabash, S. (2021). *Supplementary data for: Does Phobos reflect solar wind protons? Mars Express special flyby operations with and without the presence of Phobos.* <https://doi.org/10.5281/zenodo.5515297>
- Futaana, Y., Machida, S., Saito, Y., Matsuoka, A., & Hayakawa, H. (2003). Moon-related nonthermal ions observed by Nozomi: Species, sources, and generation mechanisms. *Journal of Geophysical Research*, *108*(A1). <https://doi.org/10.1029/2002JA009366>
- Halekas, J., Saito, Y., Delory, G., & Farrell, W. (2011). New views of the lunar plasma environment. *Planetary and Space Science*, *59*(14), 1681–1694. <https://doi.org/10.1016/j.pss.2010.08.011>

- Holmström, M., Fatemi, S., Futaana, Y., & Nilsson, H. (2012). The interaction between the moon and the solar wind. *Earth Planets and Space*, 64(2), 237–245. <https://doi.org/10.5047/eps.2011.06.040>
- Horanyi, M., Szalay, J. R., Kempf, S., Schmidt, J., Grun, E., Srama, R., & Sternovsky, Z. (2015). A permanent, asymmetric dust cloud around the Moon. *Nature*, 522(7556), 324–326. <https://doi.org/10.1038/nature14479>
- Hurley, D. M., Cook, J. C., Benna, M., Halekas, J. S., Feldman, P. D., Retherford, K. D., et al. (2016). Understanding temporal and spatial variability of the lunar helium atmosphere using simultaneous observations from LRO, LADEE, and ARTEMIS. *Icarus*, 273, 45–52. <https://doi.org/10.1016/j.icarus.2015.09.011>
- Ichimura, A. S., Zent, A. P., Quinn, R. C., Sanchez, M. R., & Taylor, L. A. (2012). Hydroxyl (OH) production on airless planetary bodies: Evidence from H<sup>+</sup>/D<sup>+</sup> ion-beam experiments. *Earth and Planetary Science Letters*, 345–348, 90–94. <https://doi.org/10.1016/j.epsl.2012.06.027>
- Ip, W. H., & Banaszekiewicz, M. (1990). On the dust/gas tori of Phobos and Deimos. *Geophysical Research Letters*, 17(6), 857–860. <https://doi.org/10.1029/g1017i006p00857>
- Jarvinen, R., Alho, M., Kallio, E., Wurz, P., Barabash, S., & Futaana, Y. (2014). On vertical electric fields at lunar magnetic anomalies. *Geophysical Research Letters*, 41(7), 2243–2249. <https://doi.org/10.1002/2014GL059788>
- Lue, C., Futaana, Y., Barabash, S., Wieser, M., Bhardwaj, A., & Wurz, P. (2014). Chandrayaan-1 observations of backscattered solar wind protons from the lunar regolith: Dependence on the solar wind speed. *Journal of Geophysical Research*, 119, 968–975. <https://doi.org/10.1002/2013JE004582>
- McComas, D., Allegrini, F., Baldonado, J., Blake, B., Brandt, P., Burch, J., et al. (2009). The Two Wide-angle Imaging Neutral-atom Spectrometers (TWINS) NASA Mission-of-Opportunity. *Space Science Reviews*, 142(1), 157–231. <https://doi.org/10.1007/s11214-008-9467-4>
- Mordovskaya, V. G., Oraevsky, V. N., Styashkin, V. A., & Rustenbach, J. (2001). Experimental evidence of the Phobos magnetic field. *JETP Letters*, 74(6), 293–297. <https://doi.org/10.1134/1.1421402>
- Mura, A., Milillo, A., Orsini, S., Kallio, E., & Barabash, S. (2002). Energetic neutral atoms at Mars 2. Imaging of the solar wind-Phobos interaction. *Journal of Geophysical Research*, 107(A10). <https://doi.org/10.1029/2001JA000328>
- Néron, Q., Poppe, A. R., Rahmati, A., Lee, C. O., McFadden, J. P., & Fowler, C. M. (2019). Phobos surface sputtering as inferred from MAVEN ion observations. *Journal of Geophysical Research: Planets*, 124(12), 3385–3401. <https://doi.org/10.1029/2019JE006197>
- Néron, Q., Poppe, A. R., Rahmati, A., & McFadden, J. P. (2021). Implantation of Martian atmospheric ions within the regolith of Phobos. *Nature Geoscience*, 14(2), 61–66. <https://doi.org/10.1038/s41561-020-00682-0>
- Ness, N. F., Behannon, K. W., Taylor, H. E., & Whang, Y. C. (1968). Perturbations of the interplanetary magnetic field by the lunar wake. *Journal of Geophysical Research*, 73, 3421–3440. <https://doi.org/10.1029/ja073i011p03421>
- Øieroset, M., Brain, D. A., Simpson, E., Mitchell, D. L., Phan, T. D., Halekas, J. S., et al. (2010). Search for Phobos and Deimos gas/dust tori using in situ observations from Mars Global Surveyor MAG/ER. *Icarus*, 206(1), 189–198. <https://doi.org/10.1016/j.icarus.2009.07.017>
- Øieroset, M., Mitchell, D. L., Phan, T. D., Lin, R. P., & Acuña, M. H. (2001). Hot diamagnetic cavities upstream of the Martian bow shock. *Geophysical Research Letters*, 28(5), 887–890. <https://doi.org/10.1029/2000GL012289>
- Poppe, A. R., Curry, S. M., & Fatemi, S. (2016). The Phobos neutral and ionized torus. *Journal of Geophysical Research: Planets*, 121(5), 770–783. <https://doi.org/10.1002/2015JE004948>
- Poppe, A. R., Fatemi, S., Garrick-Bethell, I., Hemingway, D., & Holmström, M. (2016). Solar wind interaction with the Reiner Gamma crustal magnetic anomaly: Connecting source magnetization to surface weathering. *Icarus*, 266, 261–266. <https://doi.org/10.1016/j.icarus.2015.11.005>
- Russell, C. T., & Lichtenstein, B. R. (1975). On the source of lunar limb compressions. *Journal of Geophysical Research*, 80(34), 4700–4711. <https://doi.org/10.1029/JA080i034p04700>
- Sagdeev, R. Z., & Zakharov, A. V. (1989). Brief history of the Phobos mission. *Nature*, 341(6243), 581–585. <https://doi.org/10.1038/341581a0>
- Saito, Y., Delcourt, D., Hirahara, M., Barabash, S., André, N., Takashima, T., et al. (2021). Pre-flight calibration and near-earth commissioning results of the mercury plasma particle experiment (MPPE) onboard MMO (Mio). *Space Science Reviews*, 217(5), 70. <https://doi.org/10.1007/s11214-021-00839-2>
- Saito, Y., Sauvaud, J. A., Hirahara, M., Barabash, S., Delcourt, D., Takashima, T., & Asamura, K. (2010). Scientific objectives and instrumentation of Mercury Plasma Particle Experiment (MPPE) onboard MMO. *Planetary and Space Science*, 58(1–2), 182–200. <https://doi.org/10.1016/j.pss.2008.06.003>
- Saito, Y., Yokota, S., Tanaka, T., Asamura, K., Nishino, M. N., Fujimoto, M., et al. (2008). Solar wind proton reflection at the lunar surface: Low energy ion measurement by MAP-PACE onboard SELENE (KAGUYA). *Geophysical Research Letters*, 35. <https://doi.org/10.1029/2008GL036077>
- Sauer, K., Baumgärtel, K., & Motschmann, U. (1993). Phobos events as precursors of solar wind-dust interaction. *Geophysical Research Letters*. <https://doi.org/10.1029/93gl00236>
- Schubert, G., & Lichtenstein, B. R. (1974). Observations of moon-plasma interactions by orbital and surface experiments. *Reviews of Geophysics*, 12(4), 592–626. <https://doi.org/10.1029/rg012i004p00592>
- Stern, S. A. (1999). The lunar atmosphere: History, status, current problems, and context. *Reviews of Geophysics*, 37(4), 453–491. <https://doi.org/10.1029/1999RG900005>
- Vignes, D., Mazelle, C., Rme, H., Acuña, M. H., Connerney, J. E. P., Lin, R. P., et al. (2000). The solar wind interaction with Mars: Locations and shapes of the bow shock and the magnetic pile-up boundary from the observations of the MAG/ER experiment onboard Mars Global Surveyor. *Geophysical Research Letters*, 27(1), 49–52. <https://doi.org/10.1029/1999gl010703>
- Vorburger, A., Wurz, P., Barabash, S., Wieser, M., Futaana, Y., Holmström, M., et al. (2014). First direct observation of sputtered lunar oxygen. *Journal of Geophysical Research*, 119(2), 709–722. <https://doi.org/10.1002/2013JA019207>
- Vorburger, A., Wurz, P., Barabash, S., Wieser, M., Futaana, Y., Lue, C., et al. (2013). Energetic neutral atom imaging of the lunar surface. *Journal of Geophysical Research*, 118(7), 3937–3945. <https://doi.org/10.1002/jgra.50337>
- Wieser, M., Barabash, S., Futaana, Y., Holmström, M., Bhardwaj, A., Sridharan, R., et al. (2009). Extremely high reflection of solar wind protons as neutral hydrogen atoms from regolith in space. *Planetary and Space Science*, 57, 2132–2134. <https://doi.org/10.1016/j.pss.2009.09.012>
- Wieser, M., Barabash, S., Futaana, Y., Holmström, M., Bhardwaj, A., Sridharan, R., et al. (2010). First observation of a mini-magnetosphere above a lunar magnetic anomaly using energetic neutral atoms. *Geophysical Research Letters*, 37(5). <https://doi.org/10.1029/2009GL041721>
- Witasse, O., Duxbury, T., Chicarro, A., Altobelli, N., Andert, T., Aronica, A., et al. (2014). Mars Express investigations of Phobos and Deimos. *Planetary and Space Science*, 102, 18–34. <https://doi.org/10.1016/j.pss.2013.08.002>

- Wurz, P., Rohner, U., Whitby, J. A., Kolb, C., Lammer, H., Dobnikar, P., & Martín-Fernández, J. A. (2007). The lunar exosphere: The sputtering contribution. *Icarus*, *191*(2), 486–496. <https://doi.org/10.1016/j.icarus.2007.04.034>
- Yamauchi, M., Futaana, Y., Fedorov, A., Frahm, R. A., Winningham, J. D., Dubinin, E., et al. (2011). Comparison of accelerated ion populations observed upstream of the bow shocks at Venus and Mars. *Annales Geophysicae*, *29*(3), 511–528. <https://doi.org/10.5194/angeo-29-511-2011>
- Yokota, S., Terada, K., Saito, Y., Kato, D., Asamura, K., Nishino, M. N., et al. (2020). Kaguya observation of global emissions of indigenous carbon ions from the moon. *Science Advances*, *6*(19), eaba1050. <https://doi.org/10.1126/sciadv.aba1050>